

# Quantum tunneling through planar p-n junctions in HgTe quantum wells

L. B. Zhang and Kai Chang

SKL SM, Institute of Semiconductors, Chinese Academy of Sciences, P.O. Box 912, Beijing 100083, China

X. C. Xie

Department of Physics, Oklahoma State University, Stillwater, Oklahoma 74078, USA

H. Buhmann, and L. W. Molenkamp

Physikalisches Institut (EP3), Universität Würzburg, Am Hubland, D-97074 Würzburg, Germany

(Dated: February 22, 2024)

We demonstrate that a p-n junction created electrically in HgTe quantum wells with inverted band-structure exhibits interesting intraband and interband tunneling processes. We find a perfect intraband transmission for electrons injected perpendicularly to the interface of the p-n junction. The opacity and transparency of electrons through the p-n junction can be tuned by changing the incidence angle, the Fermi energy and the strength of the Rashba spin-orbit interaction. The occurrence of a conductance plateau due to the formation of topological edge states in a quasi-one-dimensional p-n junction can be switched on and off by tuning the gate voltage. The spin orientation can be substantially rotated when the samples exhibit a moderately strong Rashba spin-orbit interaction.

PACS numbers: 78.40.Ri, 42.70.Qs, 42.79.Fm

Electrical manipulation of the transport property of topological insulators is becoming one of the central issues in condensed matter physics and has attracted rapid growing interests. Instead of symmetry breaking and a local order parameter, topological insulators are characterized by a topological invariant.[1, 2, 3] Originally, graphene was proposed as a quantum spin Hall (QSH) insulator,[4] but this turned out to be difficult to realize because the spin-orbit interaction (SOI) in this material is too small to create a gap observable in transport experiments. The QSH insulator state was proposed independently to occur in HgTe quantum wells (QWs) with inverted band structure [5, 6] and demonstrated in a recent experiment.[7] This nontrivial topological insulator[8, 9, 10, 11, 12, 13, 14] can be distinguished from an ordinary band insulator (BI) by the existence of a  $Z_2$  topological invariant.[8, 9] It possesses an insulating bulk and metallic edges, where electrons with up and down spins counter-propagate along opposite edges, and consequently shows a quantized conductance when the Fermi energy is swept across the bulk gap.[7] These topological edge states are robust against local perturbations, e.g., in purity scattering[8, 15, 16] processes and the Coulomb interaction [17, 18], and lead to novel transport properties. The low energy spectrum of carriers in QWs with inverted band structure, e.g., a TI, can be well described by a four band Hamiltonian.[5] It is highly desirable to study how to manipulate the transport properties electrically, both from a basic physics and a device application perspective.

In this Letter we investigate quantum tunneling through planar p-n junctions in HgTe QWs with inverted band structure. Perfect tunneling transmission is found

for electrons incident at normal angles. The opacity and transparency of the tunnel barrier can be controlled by tuning the angle of incidence of the charge carriers, the gate voltage (Fermi energy) and the SOI. An interesting spin refraction effect is found utilizing the strong Rashba spin-orbit interaction (RSOI) in HgTe QWs, i.e., the tunnel barrier is transparent for one spin orientation and opaque for the other. This phenomenon is difficult to be observed in a conventional semiconductor two-dimensional electron gas due to the weak SOI.[19] The quantum states in HgTe QWs consist of electron and heavy hole states and therefore show a very strong SOI which is one and even two orders magnitude than that in conventional semiconductor 2DEG, and therefore makes it possible to observe spin refraction. The topological edge channels lead to the plateau of the quantized conductance in the p-n junction sample with narrow transverse width, but the spin orientation can be rotated significantly by the RSOI. The conductance plateau can be destroyed when the QSH topological insulator is driven into the normal insulator by tuning the external electric field.

A planar p-n junction, as schematically shown in Fig. 1, can be fabricated using top gates inducing an electrostatic potential in the electron gas underneath. Electrons are injected from a nearby quantum point contact (QPC), and transmitted and/or reflected at the interface of the p-n junction. The transmitted and/or reflected electrons can be collected by other QPCs to provide further angular information. The angle of incidence of the electrons can be tuned by applying a perpendicular magnetic field.

The low energy spectrum of carriers in a HgTe QW

with inverted band structure, including the RSOI, is

$$H = \begin{pmatrix} H(k) & H_{\text{RSOI}}(k) \\ H_{\text{RSOI}}(k) & H(k) \end{pmatrix} = \begin{pmatrix} 0 & k_x + M(k) & Ak_x & ik_y & 0 & 1 \\ Ak_x & k_y & M(k) & 0 & 0 & 0 \\ ik_y & 0 & k_x + M(k) & Ak_x & 0 & 0 \\ 0 & 0 & Ak_x & k_y & M(k) & 0 \end{pmatrix}$$

where  $k = (k_x, k_y)$  is the carriers' in-plane momentum,  $D(k) = C - D(k_x^2 + k_y^2)$ ,  $M(k) = M - B(k_x^2 + k_y^2)$ ,  $k = k_x - ik_y$ , and  $A, B, C, D, M$  are the parameters describing the band structure of the HgTe QWs. Note that the insulator state characterized by the parameter  $M$ , which is determined by the thickness of HgTe QW [5] (for negative (positive)  $M$ , the QW is a TI (BI), respectively). Furthermore,  $H(k) = k^2 I_2 + d_i(k) \sigma_i$ , with  $d_1 = Ak_x$ ,  $d_2 = Ak_y$ ,  $d_3 = M(k)$ . Without RSOI, i.e.,  $p = 0$ , the eigenvalues and eigenvectors are  $\epsilon_k = \frac{M(k)^2 + A^2 k^2}{2}$ ,  $\psi_k = N (A k e^{-i\theta}; d(k) M(k))^T$ , respectively, where  $N = (A^2 k^2 + (d(k) M(k))^2)^{-1/2}$  are the normalization constants, and  $\theta$  is the incidence angle. When the RSOI is included, i.e.,  $p \neq 0$ , the eigenvalues become  $\epsilon_k = \frac{k^2}{2} + \frac{M(k)^2}{2} + A^2 k^2$ , respectively. The corresponding analytical expression of the eigenvectors with RSOI are omitted here for simplicity.

We first model the electrostatic potential of a p-n junction by a step-like potential, i.e.,  $V(x) = 0$ , for  $x < 0$ ;  $V$  for  $x > 0$ . This idealized model can give the essential features of the quantum tunneling, a more realistic smooth potential will be used in calculations aiming for comparison with experiments (see Fig. 2). We assume electrons are injected from the QPC at the left side of the junction with wave vector  $k_n^L = k_F$ , the wave function at the left side is then  $\psi_L(x < 0) = \sum_{m=1}^4 r_m^L e^{ik_m^L x \cos(\theta_m^L)} e^{ik_m^L y \sin(\theta_m^L)}$ , and at the right side  $\psi_R(x > 0) = \sum_{m=1}^4 t_m^R e^{ik_m^R x \cos(\theta_m^R)} e^{ik_m^R y \sin(\theta_m^R)}$ , where  $n(=L; R)$  is a four-component vector. The transmission  $T(\theta)$  is obtained using scattering matrix theory by matching the wave functions and the currents at the interface of the p-n junction with conserved  $p_y = k_F \sin \theta$ , i.e.,  $\psi_L(x < 0) = \psi_R(x > 0)$  and  $j_L(x) = j_R(x)$ , where  $j_{L,R}(x)$  are the current operators along the propagation direction, i.e., the x-axis,

$$j_{L,R}(x) = \frac{1}{2m} \begin{pmatrix} 0 & 2D_+ + k_x & A & i & 0 \\ A & 2D_- - k_x & 0 & 0 & 0 \\ i & 0 & 2D_+ + k_x & A & 0 \\ 0 & 0 & A & 2D_- - k_x & 0 \end{pmatrix} \psi$$

where  $D_+ = D + B$ ,  $D_- = D - B$ . Lengthy analytic expressions for the transmission  $T(\theta)$  and reflection coefficients can be obtained, but are omitted here for brevity. The conductance can be calculated by  $G = \frac{2}{R} \int_{-\pi/2}^{\pi/2} T(\theta) f(E_F) d\theta$ .

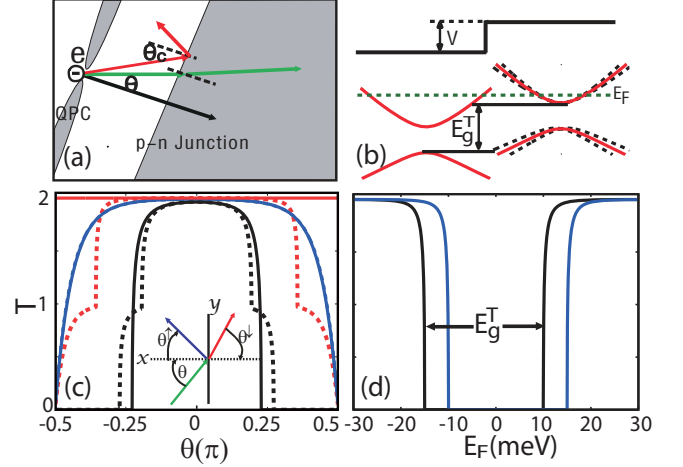


FIG. 1: (color online). (a) Schematic structure of a planar p-n junction in a HgTe QW with inverted band structure. The electric gate is positioned above the shaded region. (b) Schematic of the potential profile of the p-n junction and the band structure of HgTe QW without RSOI (red solid lines) and with RSOI (black dashed lines). The green dashed line indicates the Fermi energy.  $E_g^T$  indicates the gap in the transmission. (c) The transmission as a function of incident angle with RSOI,  $E_g = 50$  meV nm, (the dashed curves) and without RSOI,  $E_g = 0$ , (the solid curves) for a given Fermi energy  $E_F = 20$  meV.  $V_g = 5, 0, -5$  mV correspond to the blue, red and black lines, respectively. The inset shows the spin refraction schematically. (d) Transmission as a function of Fermi energy  $E_F$  for a fixed incident angle  $\theta = 0$ ,  $V_g = 5$  mV (Black line) and  $V_g = -5$  mV (Blue line).  $E_g$  denotes the bulk gap of HgTe QW. The other parameters used in the calculation are  $A = 364.5$  meV nm,  $B = 686$  meV nm,  $C = 0$ ,  $D = 512$  meV nm and  $M = 10$  meV.

Electrons incident perpendicularly to the interface can be perfectly transmitted by the p-n junction, without any backscattering, due to the unique band dispersion of HgTe QWs. This feature is caused by the helicity of the band structure, and is very similar to Klein tunneling in graphene. However, there are a number of important differences between a TI and graphene [20]: (1) the spin in the Dirac Hamiltonian of graphene denotes a pseudospin referring to the sublattices, while in a TI is a genuine electron spin; (2) In the TI, interband tunneling is suppressed because of the different energy dispersions in conduction and valence band, i.e., different group velocities. In fact, the carriers will be completely reflected when the incident angle is larger than the critical angle  $\theta_c$ . The critical angle  $\theta_c$  can be determined by Snell's law,  $\sin \theta_c = \sin \theta_R = k_F^R / k_F^L = n_R / n_L$ , and thus  $\theta_c = \arcsin(k_F^R / k_F^L)$ . An electron in the TI thus behaves as a photon which is injected from a material with larger refractive index  $n_2$  into a medium with smaller refractive index  $n_1$ . This critical angle for electrons can be tuned significantly by changing the gate voltage  $V_g$  (see the solid

curves in Fig. 1(c)), while the critical angle is difficult to change for photons. As a next step, we now include the RSOI generated by a perpendicular electric field under the electric gate (in the gray region of Fig. 1(a)). It is in principle possible to tune the potential height and the strength of the RSOI independently utilizing top- and back-gates.[21] Interestingly, the RSOI leads to a spin-dependent change of the critical angle  $\theta_c$  (see Fig. 1(c)); this is because the RSOI induces a spin splitting in the band structure, resulting in different Fermi wave vectors  $k_F$  ( $\uparrow$ ;  $\downarrow$ ) (see the solid curves in Fig. 1(b)) for the two subbands. This implies that it is possible to induce spin-dependent reflection at the p-n junction, which allows for a fully spin-polarized tunneling current when the incident angle of the electrons is tuned properly (see the inset in Fig. 1(c)), i.e.,  $\theta_{\uparrow} > \theta_{\downarrow}$ , where  $\theta_{\uparrow}$  ( $\theta_{\downarrow}$ ) is the critical angle for spin-up (-down) electron. The difference between the critical angles  $\theta_c$  with and without the RSOI can be tuned significantly by adjusting the gate voltage. This allows the realization of a spin refractive device, as a the building block for spin-optics. When we tune the Fermi energy for a fixed RSOI strength and incidence angle, the transmission exhibits a gap in which electron tunneling is forbidden; the width of the gap  $E_g^T$  corresponds to the total bulk gap of the inverted HgTe QW (see Figs. 1(b) and 1(d)). Fig. 1(d) shows that an initially opaque medium can suddenly become transparent by adjusting the Fermi level slightly. This rapid switching between opacity and transparency is a unique feature of the HgTe planar p-n junction.

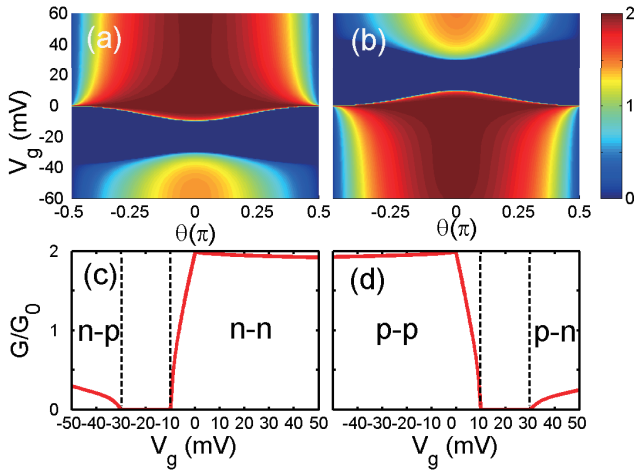


FIG. 2: (color online). (a) and (b) Contour plot for the electron transmission as function of incidence angle  $\theta$  and gate voltage  $V_g$  for Fermi energies  $E_F = 20$  meV in the ungated region, respectively. (c) and (d) Gate voltage  $V_g$  dependence of conductance  $G$  for the Fermi energy  $E_F = 20$  meV, respectively. Here the potential profile of the p-n junction is modeled by a smooth potential.

In order to see how the tunneling behavior can be controlled by adjusting the incidence angle and the Fermi en-

ergy on both sides of the junction, we show the  $\alpha$  and  $V_g$ -dependent transmission in Fig. 2. One observes clearly that perfect transmission occurs at small incidence angles  $\theta_c \rightarrow 0$  for intraband tunneling process, e.g., n-n and p-p process (see Figs. 2(a) and 2(b)). In the vicinity of the gap where the tunneling is forbidden, the critical angle  $\theta_c$  depends strongly on the gate voltage  $V_g$  that tunes the Fermi level on the right hand side of the junction. The perfect intraband transmission thus could provide us a new possible experimental method to map the band structure in the vicinity of the bulk gap. As is evident from Fig. 2(c) and 2(d), the conductance shows a strongly asymmetry behavior when comparing intraband and interband tunneling. For n-n or p-p processes, the perfect transmission leads to a large conductance while the small interband transmission, i.e., the n-p process, gives rise to a small conductance. This interesting feature are in good agreement with a very recent experiment, (Fig. 2.4 in Ref. 22) the quantitative difference comes from the simplified model used in the calculation in which the contribution from the light-hole is neglected when the Fermi energy locates at the bulk states.

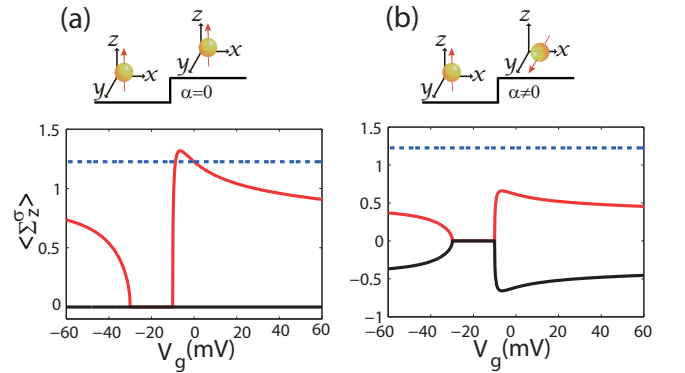


FIG. 3: (color online). The spin projection  $\langle S_z \rangle$  as a function of gate voltage  $V_g$  (in (a) and (b)) for a fixed Fermi energy  $E_F = 20$  meV and spin orientation at the left side of p-n junction, which is indicated by the dashed-blue lines. The red and black lines correspond to the spin projections  $\langle S_z \rangle$  and  $\langle S_z \rangle$  of the transmitted electron, respectively. The insets show schematically the changes of the spin orientations for the cases without (a) and with (b) RSOI, respectively. The other parameters are (a)  $\alpha = 0$ ,  $\beta = 0$ , (b)  $\alpha = 0$ ,  $\beta = 5$  meV nm, respectively.

We further investigate the spin transport properties of the p-n junction by calculating the spin projection  $\langle S_z \rangle = \langle S_{z,e} \rangle + \langle S_{z,h} \rangle$ , where  $\langle S_{z,e} \rangle$  ( $\langle S_{z,h} \rangle$ ) denotes the z-component of electron (heavy hole) spin. When the RSOI is present in the system, which, like the Fermi energy, can be tuned by voltage imposed on the structure (in the right gray region of Fig. 1(a)), the spin orientation of transmitted carriers changes greatly even for very weak RSOI ( $\beta = 5$  meV nm). For example, consider an electron injected from the left side

carrying up-spin through the p-n junction. When the RSOI is absent (see Fig. 3(a)), the gate voltage  $V_g$  only slightly changes the spin projection  $\langle \sigma_z \rangle$ . In the presence of a moderate RSOI ( $\alpha = 5 \text{ meV nm}$ ), the spin orientation of transmitted electrons becomes in-plane, since the out-of-plane component  $\langle \sigma_z \rangle = \langle \sigma_z^{\#} \rangle + \langle \sigma_z^{\#} \rangle$  vanishes due to the effective magnetic field resulting from the RSOI (see Fig. 3(b)). This demonstrates that the RSOI can substantially rotate the spin orientation.

Up to now, we only have considered two-dimensional case and ignored the contribution from the helical edge states in the region where the Fermi level is in the gap. Next, we turn to discuss the quantum tunneling through a p-n junction in a quasi-one-dimensional (Q1D) channel where the transverse modes are quantized like in a quantum point contact, but the channel width is still large enough that the helical edge states localized at opposite edges only overlap slightly. Such a Q1D QSH bar structure, which could be fabricated using standard lithographical techniques, is shown schematically in the inset of Fig. 4(a). Assuming hard-wall confinement, the wave function in the left side of the structure can be written as  $\psi_L(x < 0) = \sum_n e^{ik_n^L x} \phi_n(y) + \sum_m r_m e^{ik_m^L x} \phi_m(y)$ , emerging on the right side as  $\psi_R(x > 0) = \sum_n t_m e^{ik_m^R x} \phi_m(y)$ , where  $\phi_n(y) = \sqrt{\frac{2}{W}} \sin \frac{n\pi y}{W}$ . Using scattering matrix theory and the Landauer-Buttiker formula we can calculate the total transmission  $T$ .

The helical edge states lead to a conductance plateau at  $G = 2e^2/h$  when the Fermi energy is located within the bulk gap. When electrons tunnel through a p-n junction including edge states, perfect transmission can be observed for the intra- and inter-band tunneling processes due to the conservation of the helicity of the edge states. This perfect transmission in a Q1D system differs from that in 2D discussed above (see Fig. 2). The minigaps in Fig. 4(a) indicated by the vertical arrows in the plateau are caused by the coupling between the counter-propagating edge states in the n- and p-regions with opposite spins stemming from the opposite sides of the QSH bar. The most interesting aspect revealed by our calculation is that the conductance plateau due to the edge states is independent of gate voltage  $V_g$  due to the conservation of the helicity of the edge states. A pronounced perfect transmission feature can also be observed in the other tunneling processes, i.e., p-p, n-n, p-n and n-p junctions. In a Q1D, this feature is quite distinct from that in a 2D system (see Fig. 2). Surprisingly, the tunneling process between BI and TI, which is shown in Fig. 4(b), is very different. By tuning the band parameter  $M$  electrically, [6] the transport through the topological edge channels can be blocked for the TI/BI ( $M > 0$ ) hybridized structure and become vanishing small for the topological insulator ( $M < 0$ ) (see the insets of Figs. 4(a) and 4(b)). When the electrons are transported in a

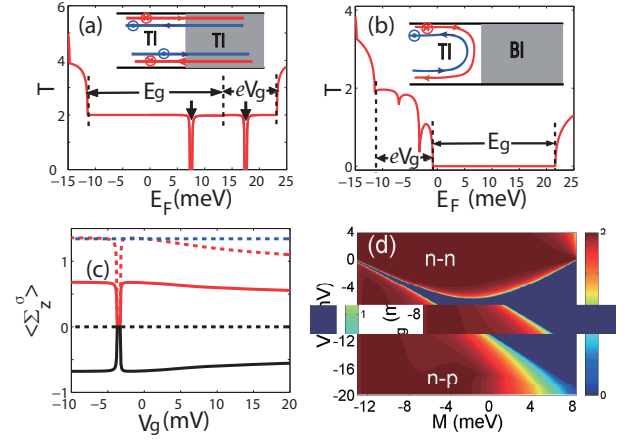


FIG. 4: (color online). (a) and (b) Fermi energy dependence of the transmission  $T$  (red line) in a QSH bar with gate voltage  $V_g = 10 \text{ mV}$  for TI-TI and TI-BI tunneling.  $E_g$  ( $eV_g$ ) denotes the gap in the bulk (the height of the potential profile of the p-n junction), ranging from  $-11 \text{ meV}$  to  $13 \text{ meV}$ . The insets show schematically the edge channels in the TI/TI and TI/BI p-n junctions in the QSH bars. (c) The spin projections  $\langle \sigma_z \rangle$  as a function of gate voltage  $V_g$  for a fixed Fermi energy  $E_F = 10 \text{ meV}$ . The dashed-blue lines denote the spin orientation of the incident electrons. The solid and dashed lines correspond to the cases with and without RSOI respectively, where the red and black curves represent the spin  $\langle \sigma_z^{\#} \rangle$  and  $\langle \sigma_z^{\#} \rangle$ . (d) Contour plot of the transmission as function of  $M$  and  $V_g$  for a fixed Fermi Energy  $E_F = 10 \text{ meV}$ . The width of the QSH bar is set at  $W = 200 \text{ nm}$ .

TI system ( $M < 0$ ), the conductance plateau does not change with gate voltage  $V_g$  except for the region of the minigaps. While for  $M > 0$ , the conductance plateau disappears totally, because the BI blocks the edge channels. This means that one can switch on/off the transport property electrically in a hybrid BI/TI system. Interestingly, the RSOI would not affect the transmission plateau since the RSOI preserves time reversal symmetry and would not destroy the edge channels. The spin orientation of the transmitted electrons can, however, be changed significantly by the RSOI, just as in the 2D case. In Fig. 4(c), one observes that the spin projection  $\langle \sigma_z \rangle$  of the transmitted electrons vanishes for spin-up injection because the RSOI behaves like an in-plane magnetic field leading to a giant spin rotation.

In summary, we have studied quantum tunneling through p-n junctions in HgTe QWs with inverted band structures. An interesting perfect transmission of the quantum tunneling process is found for electrons injected normal to the interface of the p-n junction. The opacity and transparency of the p-n junction can be tuned by changing the incidence angle of the incoming carriers, the gate voltage (which determines the Fermi level on the right hand side of the junction) and the strength of the Rashba spin-orbit interaction. Spin-up and spin-down electrons can be separated spatially utilizing the

RSOI, which could result in a building block for spin-optics. Tunneling through topological edge states can be switched on and off by tuning the band parameters electrically. This provides an efficient means of controlling the transport properties of topological edge channels electrically.

This work was supported by the NSFC Grant Nos. 60525405 and 10874175. Xie is supported by US-DOE and US-NSF. K.C. would like to appreciate Prof. R.B. Tao for helpful discussion.

---

Electronic address: kchang@red.semi.ac.cn

- [1] D. J. Thouless, M. Kohmoto, M. P. Nightingale, and M. den Nijs, *Phys. Rev. Lett.* **49**, 405 (1982).
- [2] F. D. M. Haldane, *Phys. Rev. Lett.* **61**, 2015 (1988).
- [3] X.-G. Wen and Q. Niu, *Phys. Rev. B* **41**, 9377 (1990).
- [4] C. L. Kane and E. J. Mele, *Phys. Rev. Lett.* **95**, 226801 (2005).
- [5] B. A. Bernevig, T. L. Hughes, and S. C. Zhang, *Science* **314**, 1757 (2006).
- [6] Wen Yang, Kai Chang, and S. C. Zhang, *Phys. Rev. Lett.* **100**, 056602 (2008); J. Li and Kai Chang, *Appl. Phys. Lett.* (in press).
- [7] M. König, S. Wiedmann, C. Brune, A. Roth, H. Buhmann, L. W. Molenkamp, X. L. Qi, and S. C. Zhang, *Science* **318**, 766 (2007).
- [8] C. L. Kane and E. J. Mele, *Phys. Rev. Lett.* **95**, 146802 (2005).
- [9] L. Fu and C. L. Kane, *Phys. Rev. B* **76**, 045302 (2007).
- [10] D. Hsieh, D. Qian, L. Wray, Y. Xia, Y. S. Hor, R. J. Cava, and M. Z. Hasan, *Nature* **452**, 970 (2008).
- [11] H. J. Zhang, C. X. Liu, X. L. Qi, X. Dai, Z. Fang, and S. C. Zhang, *Nat. Phys.* **5**, 438 (2009).
- [12] Y. Xia, D. Qian, D. Hsieh, L. Wray, A. Pal, H. Lin, A. Bansil, D. Grauer, Y. S. Hor, R. J. Cava, and M. Z. Hasan, *Nat. Phys.* **5**, 398 (2009).
- [13] Y. Ran, Y. Zhang, and A. Vishwanath, *Nat. Phys.* **5**, 298 (2009).
- [14] B. A. Bernevig and S. C. Zhang, *Phys. Rev. Lett.* **96**, 106802 (2006).
- [15] J. Li, R. L. Chu, J. K. Jain, and S. Q. Shen, *Phys. Rev. Lett.* **102**, 136806 (2009).
- [16] H. Jiang, S. G. Cheng, Q. F. Sun, and X. C. Xie, *Phys. Rev. Lett.* **103**, 036803 (2009).
- [17] C. Xu and J. E. Moore, *Phys. Rev. B* **73**, 045322 (2006).
- [18] C. J. Wu, B. A. Bernevig, and S. C. Zhang, *Phys. Rev. Lett.* **96**, 106401 (2006).
- [19] M. Khodas, A. Shekhter and A. M. Finkel'stein, *Phys. Rev. Lett.* **92**, 86602 (2004).
- [20] C. W. J. Beenakker, *Rev. Mod. Phys.* **80**, 1337 (2008).
- [21] J. Nitta, T. Aikazaki, H. Takayanagi, and T. Enoki, *Phys. Rev. Lett.* **78**, 1335 (1997).
- [22] M. König, Spin-related transport phenomena in HgTe-based quantum well structures, PhD thesis, Universität Würzburg (2007).